Front. Energy 2015, 9(2): 187–198
DOI 10.1007/s11708-015-0359-5

RESEARCH ARTICLE

Najet REBEI, Ali HMIDET, Rabiaa GAMMOUDI, Othman HASNAOUI

Implementation of photovoltaic water pumping system with MPPT controls

Abstract To increase the output efficiency of a photovoltaic (PV) system, it is important to apply an efficient maximum power point tracking (MPPT) technique. This paper describes the analysis, the design and the experimental implementation of the tracking methods for a standalone PV system, using two approaches. The first one is the constant voltage (CV) MPPT method based on the optimum voltage, which was deduced experimentally, and considered as a reference value to extract the optimum power. The second one is the increment conductance (IncCond) MPPT method based on the calculation of the power derivative extracted by the installation. The output controller can adjust the duty ratio to the optimum value. This optimum duty ratio is the input of a DC/DC boost converter which feeds a set of Moto-pump via a DC/AC inverter. This paper presents the details of the two approaches implemented, based on the system performance characteristics. Contributions are made in several aspects of the system, including converter design, system simulation, controller programming, and experimental setup. The MPPT control algorithms implemented extract the maximum power point (MPP), with satisfactory performance and without steady-state oscillation. MATLAB/Simulink and dSpace DS1104 are used to conduct studies and implement algorithms. The two proposed methods have been validated by implementing the performance of the PV pumping systems installed on the roof of the research laboratory in INSAT Tunisia. Experimental results verify the feasibility and the improved functionality of the system.

Keywords photovoltaic generator (PVG), maximum power point tracking (MPPT), boost DC/DC converter, DC/AC inverter, moto-pump

Received August 26, 2014; accepted December 16, 2014

Najet REBEI (✉), Ali HMIDET, Rabiaa GAMMOUDI, Othman HASNAOUI
Unit of Research (ERCO), National Institute of Applied Sciences of Tunisia, North Urban Center, University of Carthage, 1080 Tunis Cedex, Tunisia
E-mail: najet_r@yahoo.com

1 Introduction

The sources of oil are becoming increasingly rare, while the energy demands of the world rise continuously. It is estimated that global reserves will be exhausted by 2030 if consumption is not radically amended. Because of this fact, it is necessary to find another way to take over the constraint and to use a source of economic power and low emissions because the environmental protection has become an important issue [1]. Many scientific studies have been conducted in the field of unlimited energy, such as the production of electricity through wind and solar energy conversion [2,3]. So, the economic incentives and huge steps in electronic technology are promoting the use of photovoltaic systems. The solar photovoltaic energy has been a topic of interest and has made impressive progress in many countries all over the world in recent years. Specially, standalone photovoltaic pumping systems have become a favorable solution for water supply, because of more acceptance and market share, particularly in rural areas that have an important amount of illumination and have no access to an electric grid. The maximization of the energy consumption of these systems via maximum power point tracking (MPPT) has not been sufficiently exploited in practice. Directly connected systems, for example, operate at the intersection of current-voltage curves of the PV array and the moto-pump position. This operating point may be far from the maximum power point (MPP) of the generator, so it wastes a significant proportion of the available solar power. A DC/DC converter controlled by an MPPT algorithm can be used as a pump controller to match the PV generator to the optimum motor-pump position. A number of different MPPT algorithms have been proposed [4,5]. The many methods in photovoltaic applications proposed in literature can be classified into two categories, the indirect or linear method and nonlinear

or direct method. The indirect or linear method, such as constant voltage MPPT control where the voltage giving the MPP variable is usually based on a fixed ratio of the open circuit voltage or from optimal photovoltaic voltage deduced experimentally. This removes, in most cases, the MPP dependence of the temperature and illumination variation. But the accuracy of the operating voltage adjustment depends on the choice of this report. This method is extremely simple. It is just a choice of the optimal value of the ratio. There is a similar method for tracking the MPP based on short circuit current and open constant voltage. The nonlinear or direct methods include the incremental conductance (Inc-Cond) technique and the perturbation and observation (P & O) technique [6].

In this paper, two different methods are presented. The constant voltage control as an indirect method, the simplest of this technique, is to operate the PV array at a constant voltage equal to the MPP voltage (ignoring the effects of variations in light and temperature on the optimal voltage). This value is used as a reference to a feedback control loop that usually employs a PI controller to adjust the DC-DC converter duty ratio. It is realized by an analog and/or a digital circuit. The implementation efficiency is improved by employing the increment conductance MPPT technique as a direct method. This is a simple algorithm that does not require a previous knowledge of the PV generator characteristics or the measurement of solar intensity and cell temperature. The optimum voltage is instantaneously adjusted under various weather conditions. Some experimental studies which are realized on the solar panel on different days are presented where the behavior of the voltage and the current under different climate conditions are recorded. Besides, a detailed theoretical and experimental evaluation of the reference constant voltage and the increment conductance implementation techniques, in terms of overall energy utilization is also described [7–10]. Finally, the effects of the different climatic perturbation and the speed variation of moto-pump are investigated and the criteria for the choice of some parameters are proposed.

2 System description and experimental methodology

The experimental PV pumping system prototype was composed of ten 500 Wp, TITAN- 12-50/ STP-50-01 solar modules (associated into series connected modules), a boost DC/DC, a DC/AC inverter, a Sun-Pumps LOWARA CEA70/3/A which was driven by a three-phase induction Motor 3~SM63BG/304 and a dSpace DSP1104interface card which was used for acquisition, control and treatment of the results. The DC/AC inverter is a SEMIKRON type of 20 KVA power, which essentially comprises of three power modules (bridge arm SKM50GB123D), each consisting of two IGBT switches of rated current 50 A. The simplified circuit diagram of this setup is illustrated in Fig. 1

The PV array was installed to face the maximum possible annual light incidence at a fixed tilt angle. The current and voltage of the PV array were measured with LA25-NP and LV25-P, respectively. For experimental flexibility and ease of programming, a Texas instruments TMS320F240 DSP based on control kit CP1104 was used for the control and the data acquisition. The meteorological parameters were recorded utilizing a weather sensors cell (temperature and illumination) installed on the same roof on which the PV array was installed as shown in Fig. 2.

A longer experimental test was conducted to study the effects of variations of solar illumination and the variations of cell temperature on the system behavior, and to calculate the energy utilization under different weather conditions. In this test, the parameters were recorded with a low acquisition rate to limit the storage memory required for the acquisition of files. These tests were repeated many times under different weather conditions. The experimental results are shown to demonstrate the performance of the MPPT algorithm during periods of slow and smooth changes in illumination conditions, as well as faster illumination changes that occur over a period of a few seconds. Such irradiance changes are common in Tunisia where these tests were performed.

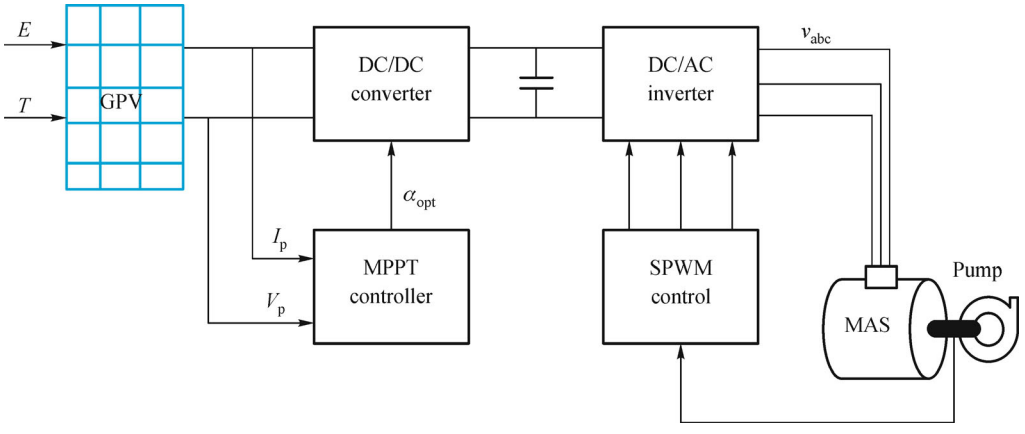

Fig. 1 Block diagram of the photovoltaic water pumping system

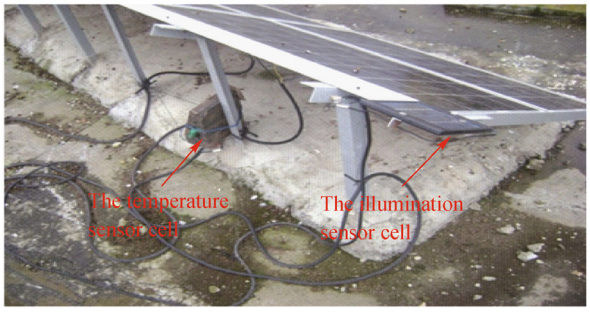

Fig. 2 Temperature and illumination sensors cells

3 Photovoltaic generator (PVG) experimental studies

The experimental results are realized with the PVG that is composed often series modules, in order to provide the desired values of the output voltage and current using

$$I_{pv} = I_{sc} - I_s\left[\exp\left(\frac{V_{pv} + r_s I_{pv}}{v_{th}}\right) - 1\right] - \frac{V_{pv} + r_s I_{pv}}{r_{sh}}, \quad (1)$$

where $I_{sc} = \frac{E_s}{E_{sr}} n_{pm}[I_{scr} + k_T(T_j - T_{jr})]$, $i_s = i_s(T_j) = i_{sr}\left(\frac{T_j}{T_{jr}}\right)^3 \exp\left(w_g\left(\frac{1}{v_{Tr}} - \frac{1}{v_T}\right)\right)$, and $v_T = \frac{K_I K_B}{q} T_j$, $v_{Tr} = \frac{K_I K_B}{q} T_{jr}$, where r indicates that the value corresponds to the standard test condition (STC) regime defined by a solar irradiance $E_{sr} = 1000\ \mathrm{W/m^2}$ and junction temperature $T_{jr} = 25°\mathrm{C}$.

3.1 Radiation influence

The following results are recorded using the illumination sensor during a few moments ignoring variations in ambient temperature within 1%. So, for an ambient temperature of 26°C, $I_{pv} = f(V_{pv})$ are gathered at different radiations during a few days as depicted in Fig. 3. The short-circuit current increases linearly with illuminations; but the open circuit voltage remains practically invariable.

3.2 Temperature influence

To record the temperature influence, the characteristics $I_{pv} = f(V_{pv})$ were collected for a few days and during diverse times. In addition, a number of characteristics that have the same illumination and various temperatures were presented. For example, Figure 4 presents the experimental results that show the $I_{pv} = f(V_{pv})$ characteristic for four different ambient temperatures (29°C, 26°C, 24°C, 23.2°C) and for a fixed illumination (600 W/m²).

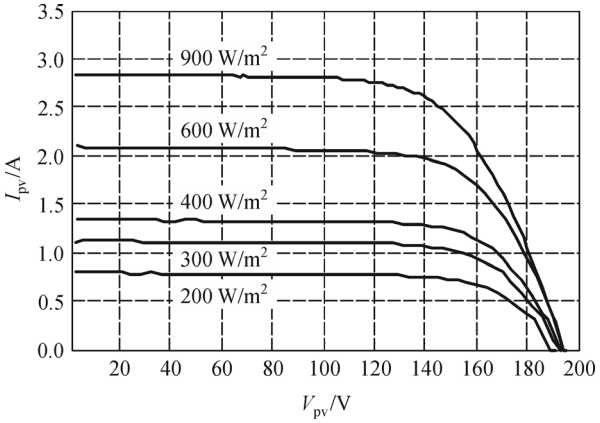

Fig. 3 *I-V* photovoltaic characteristic for different irradiation levels

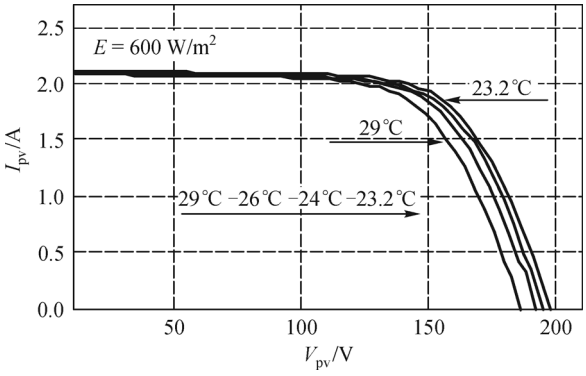

Fig. 4 *I-V* photovoltaic characteristic for different temperatures

3.3 PVG optimal operation

According to the experimental studies, the optimal characteristics of the PV generator were determined as a function of illumination and temperature. Note that the optimal PV generator voltage varies very little with the illumination. Figure 5 represents the *P-V* characteristic for different illuminations of 200 W/m², 300 W/m², 400 W/m², 600 W/m²and 900 W/m² at a fixed ambient temperature (26°C). Figure 6 gives the evolution of $P_{pv} = f(V_{pv})$ for variable ambient temperatures at a fixed illumination of 600 W/m².

The reference voltage is defined experimentally in the vicinity of 148 V and is used to extract the maximum power with a precision of 2%. Similarly, the average voltage is 148 V for different temperatures with a precision of 1.3%. The maximum power is known to have an accuracy of 2.2%. The results of these experiments show that the voltage which allows the operation at the optimal operating point (MPPT) is approximately 148 V. This voltage is selected as a reference voltage for the MPPT constant voltage control.

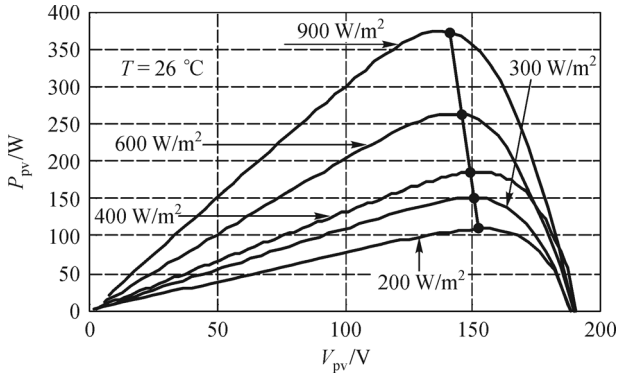

Fig. 5 *P-V* characteristic for different illuminations

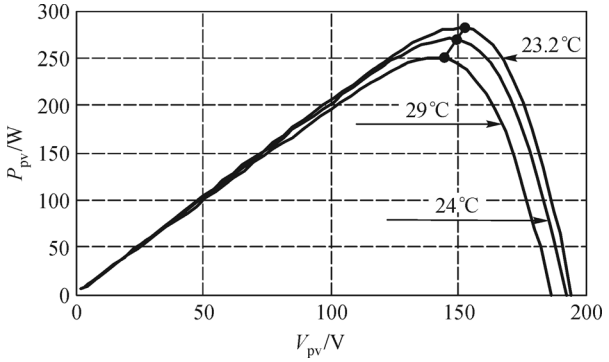

Fig. 6 *P-V* characteristic for different temperatures

4 Energy control

The electrical current provided by the solar modules as an output of the solar PV systems depends on the solar radiation on its surface and its temperature. These irregularities in the energy supply cannot be compatible with the power requirements; therefore, it is often necessary to control the supplied electricity. It is also sometimes necessary to change the nature of power for some applications (converting direct current into alternating current by an inverter). So, the insertion of a static converter is more than necessary.

4.1 DC/DC converter

To overcome the undesired effects on the power output of the PV and to extract its maximum, it is recommended that a DC/DC converter be inserted between the PV generator and the load, which can control the MPP [9]. The converter consists of a circuit topology and a control, where there will be an algorithm for MPP trackers. The role of MPPT is to ensure the operation of the PV generator at its optimum. The MPP trackers can be designed based on the boost or the buck topologies converters. The buck converter is generally used to reduce the output voltage and the boost converter is used to achieve higher output voltages. In this application, the voltage has to be increased. So the average value of the output voltage of the boost converter V_{dc} can be expressed in terms of the average value of the voltage input V_{pv} as

$$\begin{cases} V_{dc} = \dfrac{1}{1-\alpha} V_{pv}, \\ I_{dc} = (1-\alpha) I_{pv}, \end{cases} \tag{2}$$

where α is a duty cycle ratio determined by the conceived MPPT algorithm. Figure 7 demonstrates the block diagram of a boost chopper.

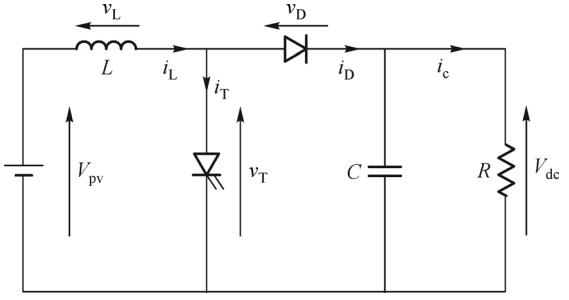

Fig. 7 Block diagram of boost chopper

4.2 Constant voltage MPPT algorithm

The constant voltage control algorithm is displayed in Fig. 8. The different blocks of the PVG output voltage regulation to its optimum (148 V) are presented in Fig. 9 and are described as:

1) An inverter amplifier which changes the sign of the reference voltage.

2) An adder converter with gain k, which calculates the error between the actual terminal voltage of the solar panel and a reference voltage, and amplifies the error. Indeed, if the voltage across the panel tends to increase, the output of the amplifier operates in the opposite direction to reduce this effect and vice versa.

3) An integrator RC with time constant τ, which provides at its output a variable slowly voltage.

4) A comparator that compares the slowly variable voltage (RC integrator) to a triangular signal for generating a modulated pulse width. This signal is supplied to the gate of the MOSFET through a MOS driver.

The tests results conducted with the MPPT control were realized in the research laboratory for two cases: both for negative error and positive one. The error (ε), the triangular signal (V_t) and the control signal (V_c) are presented. Note that $\varepsilon = V_{ref} - V_{pv}$. If $V_{ref} < V_{pv}$, thus $\varepsilon < 0$ and $-k\varepsilon > 0$ as seen in Fig. 10. V_{pv} has to be adjusted to V_{ref} to increase I_{pv}. So α has to be increased according to the following relationship:

$$I_{pv} = \frac{I_{dc}}{1-\alpha}$$

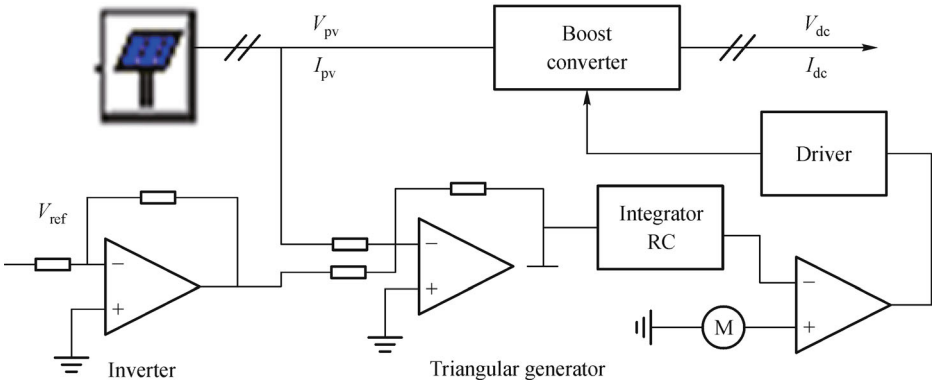

Fig. 8 Block diagram of constant voltage MPPT control

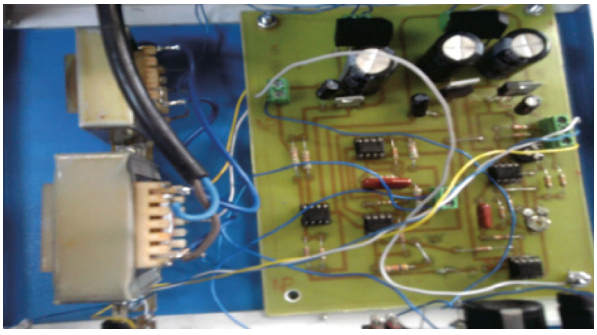

Fig. 9 Circuit of MPPT controller

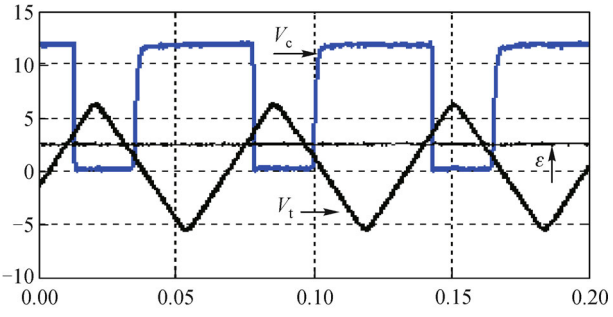

Fig. 11 Constant voltage MPPT control results with positive error

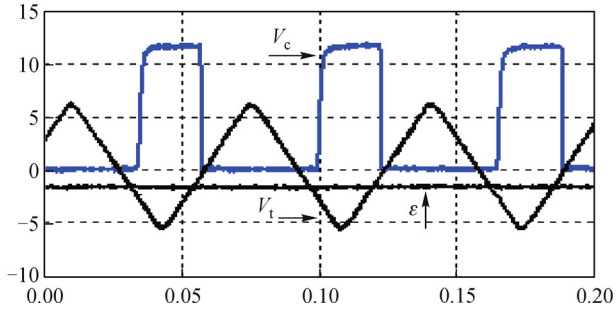

Fig. 10 Constant voltage MPPT control results with negative error

to oscillate about the optimum operation. If $V_{ref} > V_{pv}$, $\varepsilon > 0$ and $-k\varepsilon < 0$ as shown in Fig. 11. V_{pv} has to be adjusted to V_{ref} to decrease I_{pv} and thereby decrease α.

4.3 Inc-Cond MPPT algorithm

The track of the MPP was performed with another technique which gives rise to the Inc-Cond algorithm [9]. The PVG output voltage was continuously adjusted according to its optimum voltage. The basic principle of this algorithm is to calculate the derivative of the power extracted from the installation. The main operation done by this algorithm is to compare the ratio dI_{pv}/dV_{pv} to I_{pv}/V_{pv}. With reference to the comparison result, the reference signal will be adjusted in order to move the output voltage toward the MPP voltage, as shown in Fig. 12.

The derivative is equal to zero at the MPP, positive on its left and negative on its right [8]. Since the PVG power is

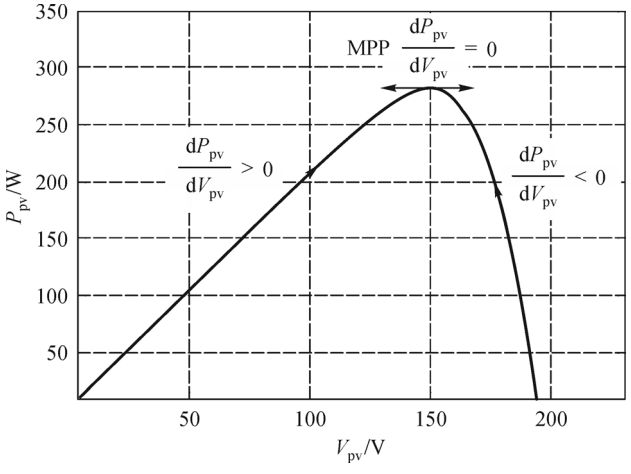

Fig. 12 Behavior of INC MPPT algorithm in thee-level operation

described by $P_{pv} = V_{pv}I_{pv}$, its derivative as a function of the voltage is then defined by Fig. 13.

5 Moto-pump fed by a GPV

The induction motor was fed from a voltage source DC/AC inverter (VSI) supplied by a PV generator with the MPP tracker. The VSI was controlled according to the well-known space vector pulse width modulation (SVPWM) technique. The magnitude of induction machine voltage is expressed by

$$V_s = \rho V_{dc} = \frac{\rho}{-\alpha} V_{pv} = \delta V_{pv} \tag{3}$$

where ρ is the voltage ratio $\rho = \dfrac{\sqrt{2}V_{ref}}{V_{dc}}$ and α is the duty ratio adjusted by the MPPT control.

The reference voltage modulus must remain inside the circle circumscribed in the hexagon of active voltage vectors of the inverter, which leads to

$$V_{ref} \leqslant \frac{V_{dc}}{\sqrt{2}}. \tag{4}$$

The study of the induction motor in a steady-state is usually performed in the case when it is powered by a sinusoidal alternating balanced three-phase voltage. The supply voltage is given by

$$V_s \cong \Phi_s \omega_s. \tag{5}$$

It should be noted here that the law $V_s/f_s = cst$ is reduced to a constant flux operation. To keep the flux constant at its nominal value, generally, the stator voltage must be adjusted in proportion to the supply frequency.

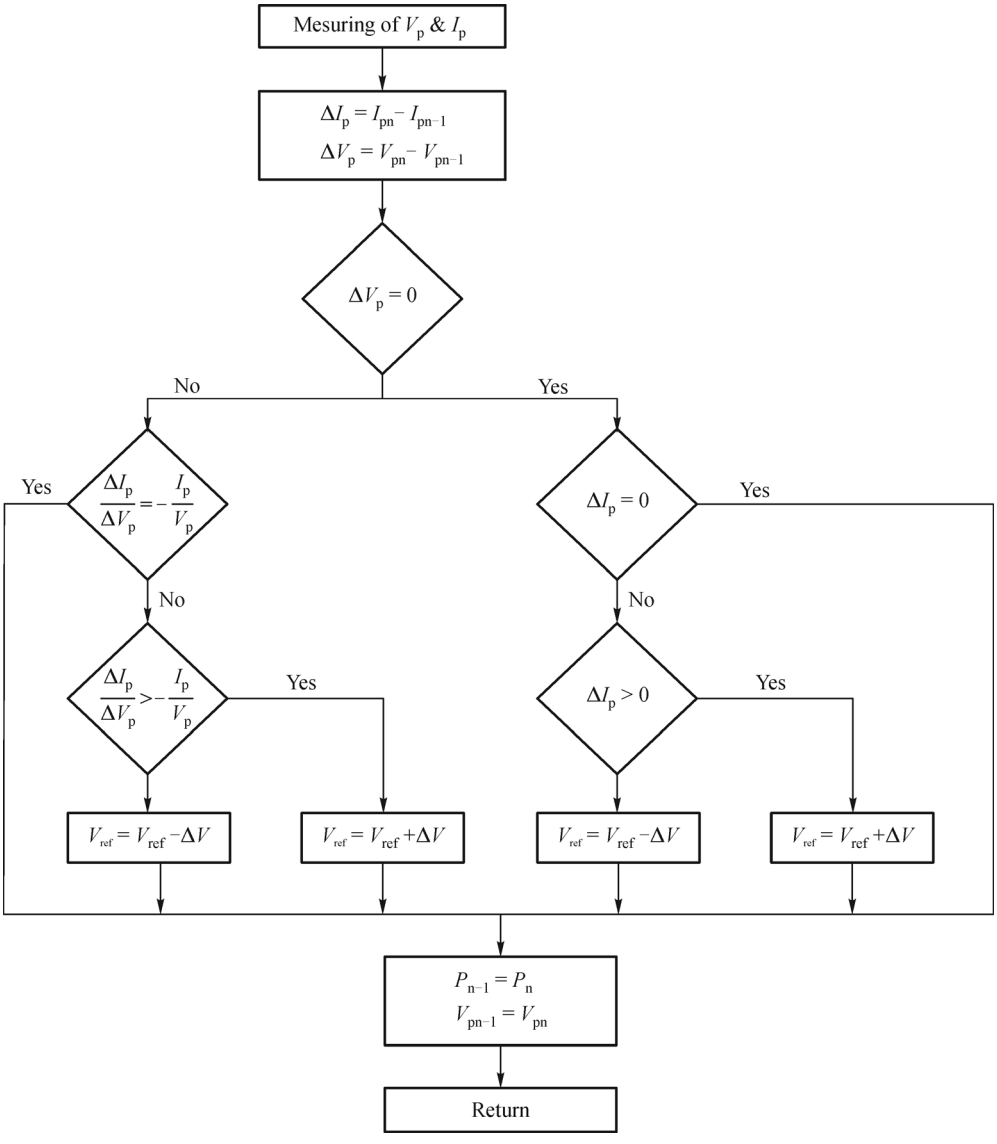

Fig. 13 Flowchart of Inc-Cond algorithm

This is the simplest approach to control the speed of induction motors, called Constant Volts/Hertz method. In addition to the electrical quantities treatment in the selected reference mark, the following mechanical model is taken into account. The variables T_e and T_L are respectively the electromagnetic and the mechanical torques.

$$\frac{d\omega_r}{dt} = \frac{p(T_e - T_L)}{J}, \tag{6}$$

where $T_e = -p\mathrm{Im}\left(\overline{\Phi_s}\overline{I_s}^*\right)$, and Im is the imaginary part of the stator flux in the complex landmark.

At the steady-state, electromagnetic torque equilibrates the mechanical torque of the load coupled to the shaft of the motor. T_L is linked to rotor speed ω_r. For simulation tests, Equation (7) was used.

$$T_L = T_L(\omega_r) = T_{L0} + T_{L1}\omega_r + T_{L2}\omega_r^2. \tag{7}$$

where T_L is the hydrodynamic load torque of the centrifugal pump which is also described by an $H(Q)$ characteristic given by

$$H = A_1\omega_r^2 - A_2\omega_r Q - A_3 Q^2. \tag{8}$$

In the case in this paper, H = 1 m. The constant coefficients of Eqs. (7) and (8) were determined from experimental tests.

$T_{L2} = 1.217e^{-5}$, $T_{L1} = 9.917e^{-5}$, and $T_{L0} = 5.939e^{-5}$;
$A_1 = 0.039$, $A_2 = -0.3079$, and $A_3 = -0.0024$.

The water flow was measured by a flow sensor installed at the outlet of the pump, as shown in Fig. 14.

Fig. 14 Experimental system

6 Experimental results

The photovoltaic water pumping system employing constant voltage and Inc-Cond MPPT algorithms is continually subjected to two excitations sources, one originating from variations in solar irradiance for a constant flux, and the other from the variation of electrical speed to study the load variation influence when the system is operating under steady-state solar irradiance. To validate the proposed approaches, a number of experiments were conducted with the proposed system as depicted in Fig. 1. Different measurements were performed during a day, when the climatic conditions were changeable. All results of optimization of the photovoltaic water pumping system were collected and presented. All parameters of the components system were described in the Appendix 1, 2 and 3. Figure 15 presents the program of the water pumping system installed on Dspace DS1104.

6.1 Maximum power transferred to the pump at variable irradiation with constant flux

It should be noted here that the law $V_s/f_s = cst$ operates at a constant flux. The imposed flux is equal to its nominal value (0.69 Wb) for a supply voltage of 220 V with a nominal speed of 314 rad/s so that the moto-pump can operate.

6.1.1 Constant voltage MPPT control results

An actual scenario of illumination that happens on the solar panel and the duty ratio which changes with illumination were recorded and presented in Fig. 16.

Figure 17 gives the evolution of the PVG voltage and the load voltage. Despite the illumination variation, the constant voltage MPPT control shows its robustness; so the PVG output voltage is maintained at its optimum around of 148 V. Figure 18 shows the displacement of the MPP. This point moves at a constant voltage.

The pump operates at a constant flux. Figure 19 shows that V_s and ω_s follow the same variation as the illumination, since V_s is related to V_{dc} by the duty ratio. Figure 20 gives the simultaneous evolution of the electromagnetic torque and the flow rate; it is clearly observed that these two variables move in the same direction as the illumination.

Figures 21 and 22 respectively represent photovoltaic current, direct and quadratic currents components of the machine.

The maximum power tracks illumination changes. For a value of 1090 W/m^2 as it is recorded in Fig. 16, the extracted power is approximately 310W, as shown in Fig. 17, and the efficiency value of the MPPT tracker is approximately 0.9626. For a decrease in the illumination of 490 W/m^2, the maximum power is approximately 180W. Thus, when the illumination further reduces, it is assumed that the system would not pump water. With the constant voltage MPPT control, the temperature effect is not involved in its progress, and in some cases, it seems a major drawback, especially when there are very low temperatures. So there will be a risk to lose a considerable amount of the optimal extracted power, since the voltage decreases when the temperature increases.

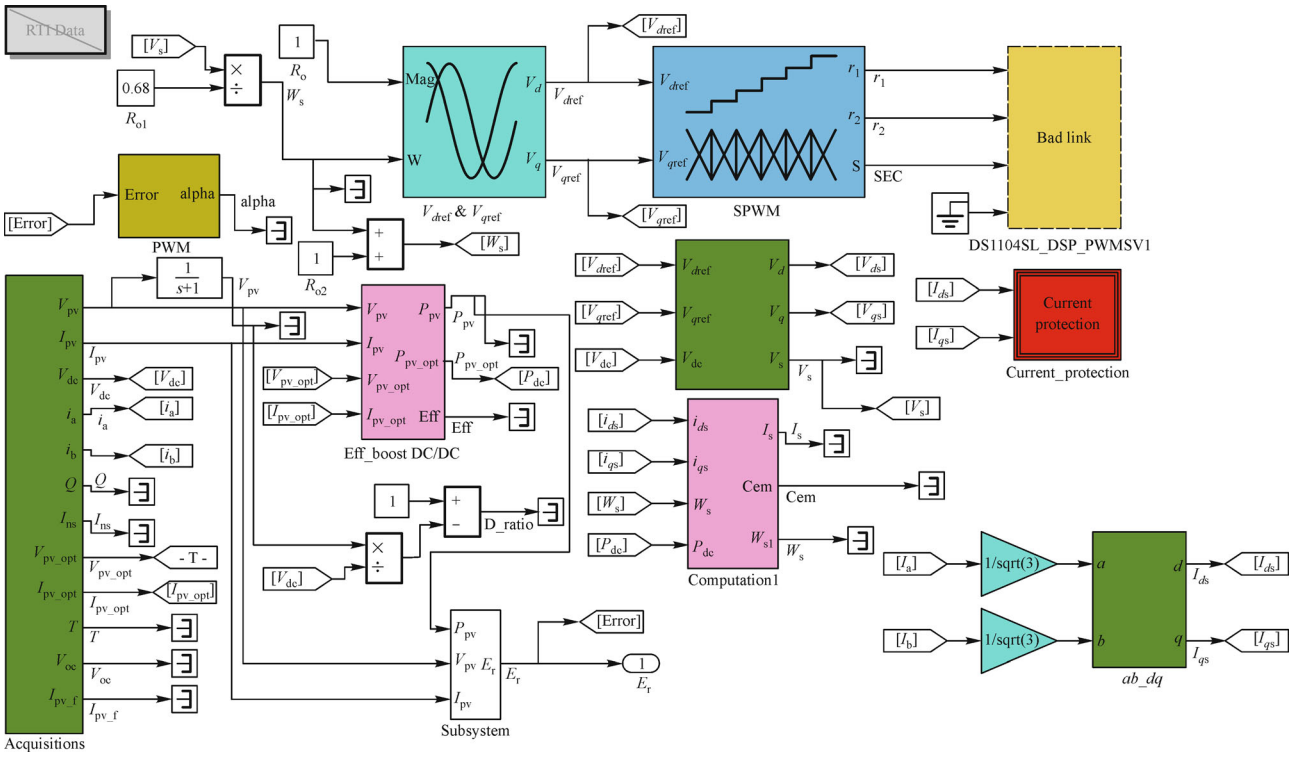

Fig. 15 Water pumping program installed on Dspace DS1104

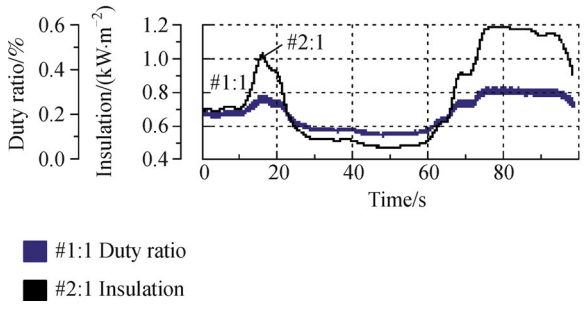

Fig. 16 Actual captured illumination and duty ratio evolution

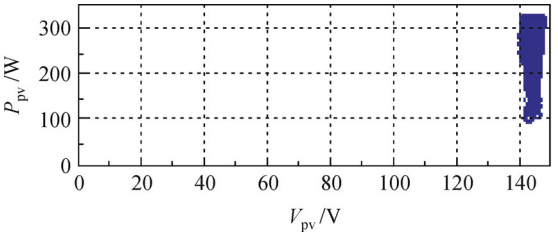

Fig. 18 Evolution of MPP

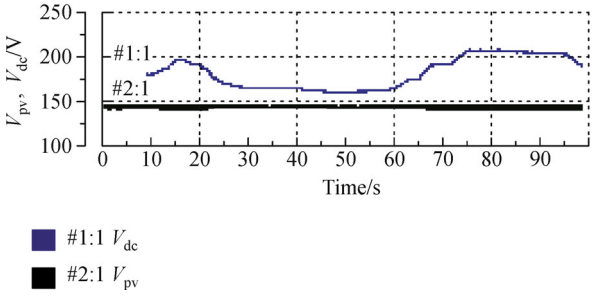

Fig. 17 PVG and load voltages

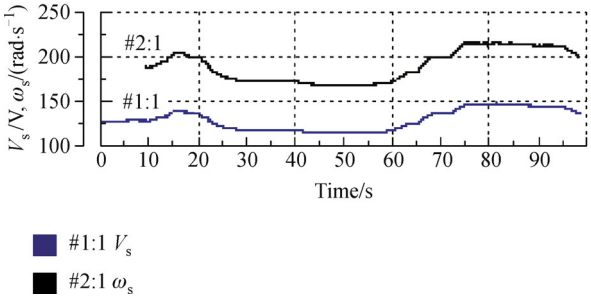

Fig. 19 Waveform of stator speed and average value V_s

6.1.2 Inc-Cond MPPT control responses

To test the incremental conductance approach, an actual randomly scenario of illumination was captured, on 14 September 2013, as shown in Fig. 23. The evolution of some physical variables was recorded. Figure 24 represents the implemented program of the Inc-Cond MPPT algorithm.

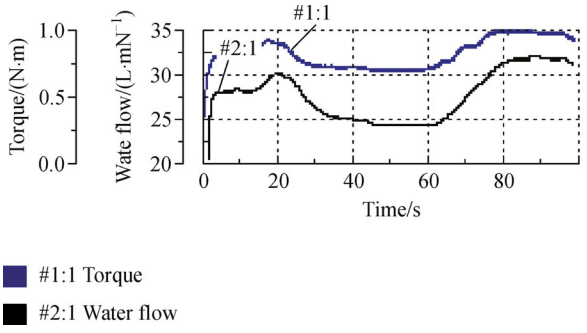

Fig. 20 Flow rate and torque evolution

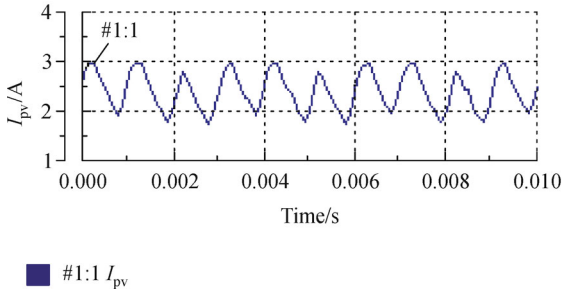

Fig. 21 Photovoltaic current waveform

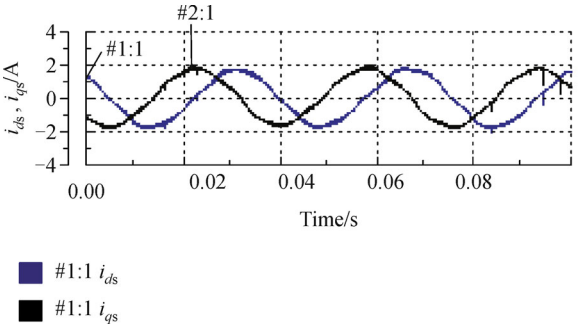

Fig. 22 Direct and quadratic currents components

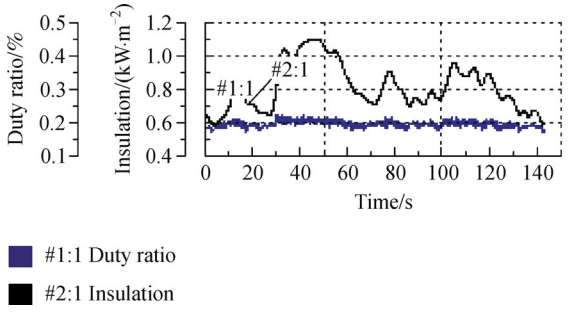

Fig. 23 Illumination and duty ratio evolution

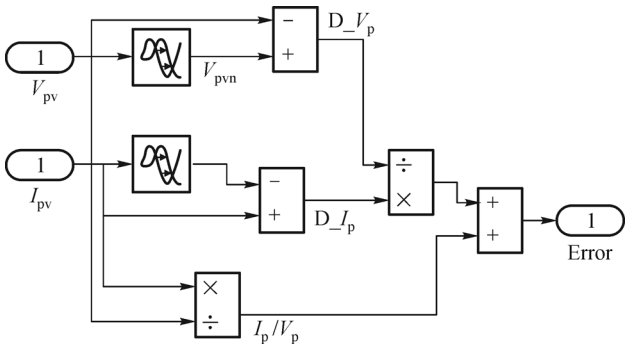

Fig. 24 Inc-cond MPPT method structure

As it is presented in Fig. 25, the PVG output voltage is continuously adjusted according to its optimum value, which is in the vicinity of 150 V, confirming that the operating point is at a maximum power. Figure 26 gives the displacement of the MPP, which is influenced by the climatic conditions that explains the oscillation of the MPP around its optimum.

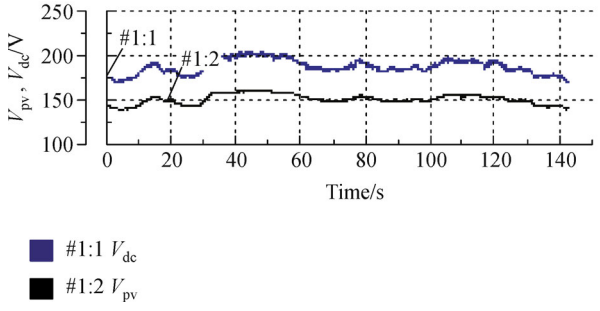

Fig. 25 Waveform of reference and output voltage

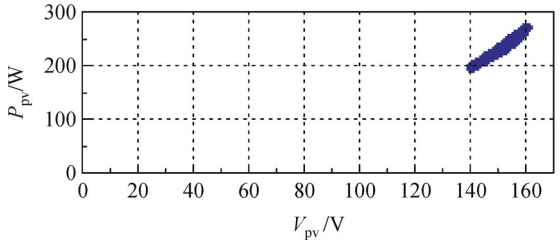

Fig. 26 Evolution of MPP with weather variation

Figure 27 exhibits the evolution of the electromagnetic torque and water flow. These two variables vary according to the climatic changes, especially according to the illumination which acts directly on the duty ratio.

From the experimental results, it is observed that the efficiency presents a more favorable value of approximately 0.982 and the extracted PVG power can reach 316 W.

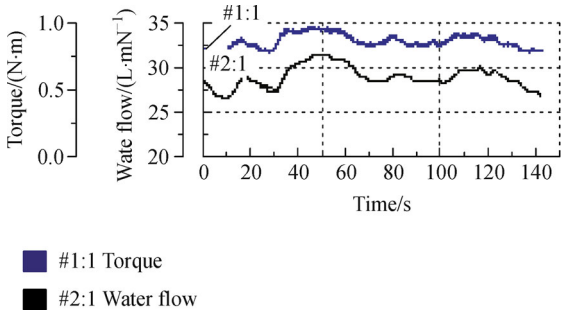

Fig. 27 Water flow rate and torque evolution

6.2 Maximum solar energy transferred to the pump at variable speed

6.2.1 Constant voltage MPPT control results

For the constant voltage control, an output reference voltage, which is equal to the optimum value of the solar panel, was used in conjunction with the controller to adjust the duty ratio. In order that the moto-pump can operate the nominal value of the flux was imposed. The speed was chosen not to exceed 314 rad/s with a variation ranging between –31.4 rad/s and +31.4 rad/s, as shown in Fig. 28. The illumination was recorded and applied around 887.75 W/m^2.

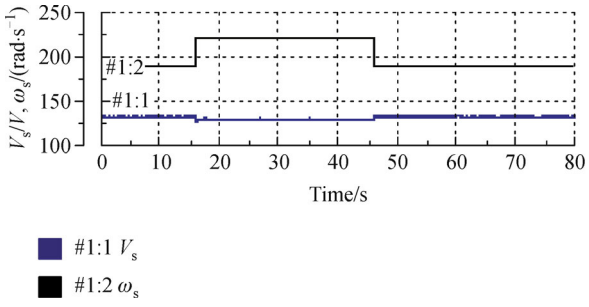

Fig. 28 V_s and ω_s evolution

Figure 29 shows the captured illumination that is nearly constant for a short period of time. Figure 30 illustrates the reference voltage which is approximately148 V and the output DC/DC converter voltage.

As illustrated in Fig. 31, the MPP is around a constant value independent of the weather variations, with small oscillations around its optimum. Figure 32 represents the evolution of the electromagnetic torque and the water flow rate. It is observed that the two variables vary with the electric speed.

6.2.2 Inc-Cond MPPT control results

The illumination was recorded for a brief moment to guarantee that it was constant, around 935.724 W/m^2. All

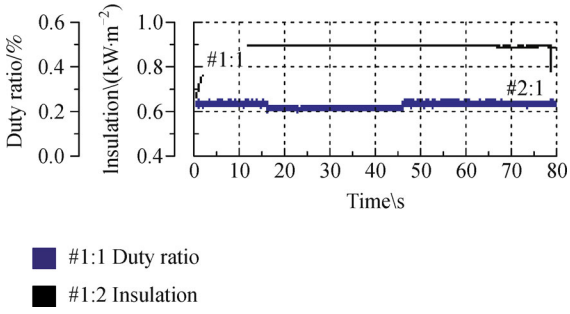

Fig. 29 Illumination and duty ratio evolution

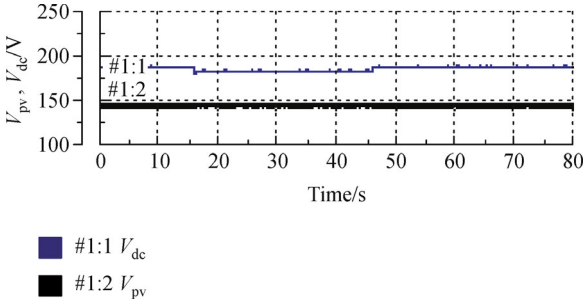

Fig. 30 Reference and output voltage waveform

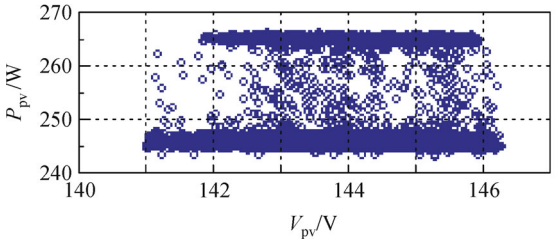

Fig. 31 Evolution of MPP

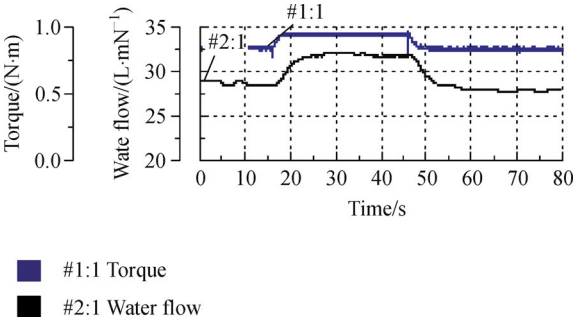

Fig. 32 Flow rate and torque evolution

quantities were registered in 50 s. The scenario of the electric speed was chosen with a step variation of 31.4 rad/s, as shown in Fig. 33.

Figure 34 shows the captured constant illumination and

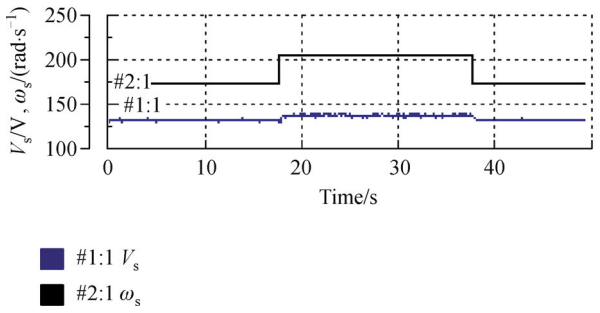

Fig. 33 ω_s and average stator voltage evolution

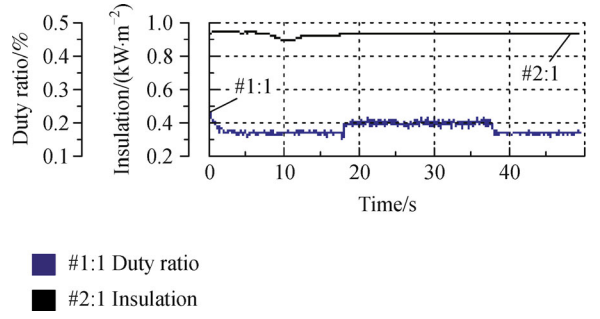

Fig. 34 Illumination and duty ratio evolution

the duty ratio evolution which changes with the imposed speed. As shown in Fig. 35, the photovoltaic voltage can attain 150 V with the Inc-Cond MPPT control. Moreover, the output boost converter voltage evolves with the duty ratio.

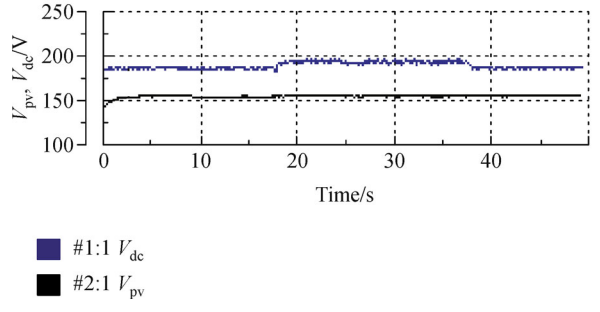

Fig. 35 PVG and load voltage wave form

As shown in Fig. 36, the MPP evolves between 140 V and 155 V. Figure 37 represents the evolution of the electromagnetic torque and the water flow rate, which vary with the speed.

To investigate the robustness of the two algorithms with respect to various random and real environmental conditions, an original set of tests were defined. These tests were conducted by recording some results from the photovoltaic station during the day independently from the climatic variations and from being connected to the water pumping system. With the two MPPT algorithms presented in this

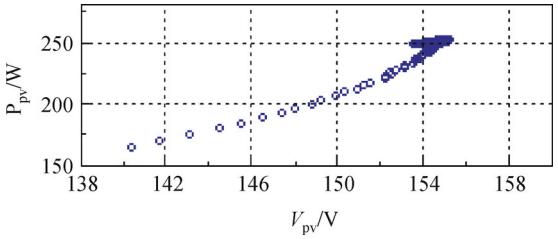

Fig. 36 MPP evolution

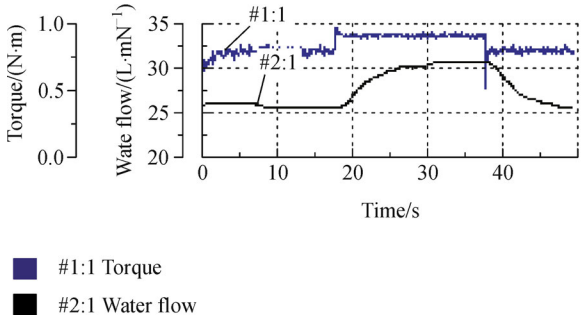

Fig. 37 Flow rate and torque evolution

work, it is noted that the functioning point always follows. Besides, the performance of the boost converter that can reach a good efficiency of nearly 0.98% for the Inc-Cond algorithm, and around 0.96% for the constant voltage algorithm. The MPPT trackers conceived in an experimental prototype were verified with the photovoltaic water pumping system. The Inc-Cond control gives, for captured illumination of approximately 935.724 W/m^2, a constant voltage which attains 154.725 V.

So it presents a better efficiency for rapid changes and a better stability when the maximum power is achieved. However, the MPPT constant voltage control is used in practice due to its simplicity but the temperature variation has no influence on optimum voltage.

The originality and the specificity of the presented results obtained during this research reside in the fact that a vital implementation of the water pumping powered with photovoltaic generator is realized. It has become an important and economical viable photovoltaic application. It is a particularly valuable application from an educational perspective due to the challenges associated with designing a system that involves direct interfacing of photovoltaic panels to a load without the inclusion of energy storage.

7 Conclusions

In this paper, a stand-alone PVG system for water pumping application was successfully implemented. The Inc-Cond and constant voltage control algorithms were used for MPPT. The results validate the MPPTs control i-

mplemented in real time application in research laboratory. The MPPT control could significantly increase the efficiency of energy production from the PVG and the performance of the PV water pumping system. The MPP was reached by any irradiation levels and for any temperatures or variations of them or other variations. The experiment results prove positively that constant voltage control and the Inc-Cond MPPTs can reach the intended MPP. Nevertheless, the approach and the stability of the MPP are not achieved within the same manner.

Notations

A_p	Pump torque constant
E_s	Illumination
H	Total pump head
I_{pv}	PVG current
I_{sc}	Photocurrent
I_{sr}	Reverse saturation current
J	Total inertia
p	Pole pairs
q	Electron charge
Q	Water flow rate
r_s	Series resistance of the PVG
r_{sh}	Shunt resistance of the PVG
T_a	Absolute temperature
T_e	Electromagnetic torque
T_L	Load torque
T_j	Junction temperature/K
V_{pv}	PVG voltage
v_{th}	Thermal voltage of the PVG
V_s	Stator voltage
K_B	Boltzmann constant
K_I	Non-ideality coefficient
Φ_s	*d-q* axis stator flux
ω_s	Synchronous angular speed
ω_r	Drive angular speed

Appendix 1 PVG parameters

P_c/W	I_{opt}/A	V_{opt}/V	V_{oc}/V	I_{sc}/A	Number of cell	Type of cell	Efficiency/%
50	2.9	17.2	21	3.4	36	Polycrystallin	11.3

Appendix 2 Pump parameters

Rated power	$P_n = 0.37\,\text{kW}$
Rated flow	$Q(\text{l/mn}) = 30(\text{min}) - 80(\text{max})$
High	$12.8(\text{min}) - 20.1(\text{max})$

Appendix 3 Parameters of induction motor

Rated power	$P_n = 0.61\,\text{kW}$
Stator resistance	$R_s = 17.68\,\Omega$
Rotor resistance	$R_r = 19.1\,\Omega$
Stator inductance	$L_s = 0.6877\,\text{H}$
Rotor inductance	$L_r = 0.6811\,\text{H}$
Mutual inductance	$M = 0.65611\,\text{H}$
Moment of inertia	$J = 0.0001\,\text{kg}\cdot\text{m}^2$
Rated torque	$T_n = 1.9\,\text{N}\cdot\text{m}$
Rated voltage	$V_n = 220\,\text{V}$
Rated current	$I_n = 1.45\,\text{A}$
Number of poles	$p = 1$

References

1. Bose B K. Global warming: energy, environmental pollution and the impact of power electronics. IEEE Industrial Electronics Magazine, 2010, 4(1): 6–17
2. Yousif C I. Recent developments of applying solar photovoltaic technologies in Malta. In: Proceedings of the Enemalta 25th Anniversary Conference on Energy Efficiency. Valetta, Malta, 2002
3. Azzouzi M. Comparison between MPPT P&O and MPPT fuzzy controls in optimizing the photovoltaic generator. International Journal of Advanced Computer Science and Applications, 2012, 3 (12): 57–62
4. Omole A. Analysis, modeling and simulation of optimal power tracking of multiple-modules of paralleled solar cell systems. Dissertation for the Master's Degree. Tallahassee: The Florida State University, 2006
5. Vaigundamoorthi M, Ramesh R. Experimental investigation of chaos in input regulated solar PV powered cuk converter. International Journal of Computer Applications (0975–8887), 2012, 43(10): 11–16
6. Rebei N, Hmidet A, Gammoudi R, Hasnaoui O. Experimental implementation techniques of P&O MPPT algorithm for PV pumping system. In: The 11th International Multi-conference on Systems, Signals & Devices (SSD'2014). Barcelona, Spain, 2014, 1–6
7. Otieno C A, Nyakoe G N, Wekesa C W. A neural fuzzy based maximum power point tracker for a photovoltaic system. In: IEEE AFRICON'2009. Nairobi, Kenya, 2009, 1–6
8. Knopf H. Analysis, simulation and evaluation of maximum power point tracking (MPPT) methods for a solar powered vehicle. Dissertation for the Doctoral Degree. Portland: Portland State University, 1999
9. Najet R, Belgacem B G, Othman H. Modeling and control of photovoltaic energy conversion connected to the grid. Frontiers of Energy and Power Engineering in China, 2012, 6(1): 35–46
10. Salameh Z M, Dagher F, Lynch W A. Step-down maximum power point tracker for photovoltaic systems. Solar Energy, 1991, 46(5): 279–282